MILKY WAY

# A three-dimensional map of the Milky Way using classical Cepheid variable stars

Dorota M. Skowron[1]*, Jan Skowron[1], Przemek Mróz[1], Andrzej Udalski[1]*, Paweł Pietrukowicz[1], Igor Soszyński[1], Michał K. Szymański[1], Radosław Poleski[1,2], Szymon Kozłowski[1], Krzysztof Ulaczyk[1,3], Krzysztof Rybicki[1], Patryk Iwanek[1]

**The Milky Way is a barred spiral galaxy, with physical properties inferred from various tracers informed by the extrapolation of structures seen in other galaxies. However, the distances of these tracers are measured indirectly and are model-dependent. We constructed a map of the Milky Way in three dimensions, based on the positions and distances of thousands of classical Cepheid variable stars. This map shows the structure of our Galaxy's young stellar population and allows us to constrain the warped shape of the Milky Way's disk. A simple model of star formation in the spiral arms reproduces the observed distribution of Cepheids.**

Cepheid variable stars pulsate, causing their brightness to vary with periods of 1 to 100 days. Classical Cepheids are young (<400 million years old) supergiant stars, whereas other types of Cepheids (type II and anomalous) arise in older stellar populations. The intrinsic luminosities of classical Cepheids span the range of 100 to 10,000 solar luminosities ($L_\odot$). This is bright enough to be detected at extragalactic distances and, within our Galaxy, through obscuring interstellar clouds of gas and dust in the foreground. Cepheids follow a pulsation period–luminosity (P-L) relation (*1*), allowing the absolute magnitude of a Cepheid to be inferred from its period. The distance can then be determined by comparing the absolute and the apparent magnitude, provided the foreground interstellar extinction is known. At optical wavelengths, interstellar extinction is often large and highly variable, but observations in infrared (IR) bands reduce these uncertainties. Detection of Cepheids in the optical bands is straightforward owing to their characteristic sawtooth-shaped light curves and large amplitudes. In the IR, the light curve shape becomes more sinusoidal and difficult to distinguish from other types of variable stars. Cepheids can appear indistinguishable from other variable stars in the optical bands if the number of measurements is limited (below 80 to 100 epochs) and the survey time span is short.

We analyzed data for 2431 galactic Cepheids, most of which were discovered by the fourth phase of the Optical Gravitational Lensing Experiment (OGLE-IV) project (*2*). This is a long-term survey of the galactic disk and Galactic Center focused on the discovery and classification of variable stars. The OGLE Collection of Galactic Cepheids (*3*) more than doubled the number of known galactic classical Cepheids. The magnitude range of the galactic plane portion of OGLE-IV, 11 to 18 mag in the *I*-band, enables identification of Cepheids as distant as the expected boundary of the galactic disk [~20,000 parsecs (pc) from the Galactic Center]. OGLE has covered almost all the galactic disk visible from its site at Las Campanas Observatory, Chile (Fig. 1).

Cepheids closer than 4 kpc are too bright, so they saturate in the OGLE survey images. Therefore, we complemented the OGLE sample with brighter objects from the list of galactic Cepheids (*4*), themselves mostly from the General Catalogue of Variable Stars (GCVS) (*5*) and the All Sky Automated Survey (ASAS) (*6*). We also supplemented the list with Cepheids discovered by the All-Sky Automated Survey for Supernovae (ASAS-SN) survey (*7*) and we identified Cepheids in the Asteroid Terrestrial-Impact Last Alert System (ATLAS) survey catalog (*8*). We also investigated Cepheid candidates from the Gaia Data Release 2 (Gaia DR2) catalog (*9*), confirming 211 of them as classical Cepheids. Full details on the sample selection are provided in (*10*).

Most of the Cepheids lie close to the galactic plane, so they are affected by extinction by dust, which is also concentrated in the plane. To reduce the effect of dust extinction, we determined the distances to individual Cepheids based on mid-IR photometry obtained by the Spitzer and Wide-field Infrared Survey Explorer (WISE) satellites corrected for interstellar extinction (*10*), as well as appropriate P-L relations (*11*). Positions and distances of each Cepheid were converted to Cartesian coordinates with the Sun at the origin to facilitate study of their three-dimensional distribution (*10*).

Figure 1 presents our map of the Galaxy in Cepheids, representing the young stellar population. We show the view projected on the sky (Fig. 1A) and face-on (Fig. 1B), together with a four-arm spiral galaxy model consistent with neutral hydrogen (H I) observations (*12*). Areas of higher Cepheid density indicate the nonuniform galactic structure or regions of enhanced star formation. The side view (Fig. 1A) shows that the young stellar disk of the Milky Way between longitudes $240° < l < 330°$ lies below the galactic plane (as traced by Cepheids), which suggests warping of the galactic disk.

We subdivided the Galaxy into 12 sectors of unequal azimuthal width in the galactocentric polar coordinate system with the azimuth $\phi = 0°$ pointing to the Sun (Fig. 2A). The disk is not flat; the warp is evident in directions that are sufficiently well populated with Cepheids (Fig. 2B). The warping of the disk begins at a distance of ~8 kpc and becomes steeper at ~10 kpc, reaching out to the edge of the Galaxy at ~20 kpc. The disk warps toward negative distance from the galactic plane ($Z$) in the azimuth range $0° < \phi < 135°$ and toward positive $Z$ in the range $165° < \phi < 330°$, although the exact boundary is unclear because of the smaller number of known Cepheids on the far side of the Galactic Center. To further illustrate the warping of the disk and as a guide to the eye, we fitted a simple model surface to the Cepheid distribution (*10*); this is shown in Fig. 2, C to E, from three viewing angles.

The warping of the disk has been observed before, in H I (*12*, *13*), stars (*14*–*18*), dust (*19*), and kinematics of stars in the plane of the sky (*20*, *21*). Our map shows the warp in three dimensions and differs from models derived from those earlier detections (*10*).

We modeled the thickness of the young disk by fitting a simple exponential model (*10*). We measured the disk scale height within the solar orbit, $H = 73.5 \pm 3.2$ pc, and the distance of the Sun from the galactic plane, $z_0 = 14.5 \pm 3.0$ pc (fig. S3). These values can be compared to the past determinations (table S2). We removed the average warp shape from the galactic disk to analyze its flaring properties far from the center (fig. S2). We found that the flaring of the disk in Cepheids matches that seen in neutral hydrogen (*22*) (fig. S2B).

The distribution of classical Cepheid pulsation periods as a function of the distance from the Galactic Center is shown in fig. S4. It shows a decrease in the minimal pulsation periods of Cepheids with increasing galactocentric distance, consistent with a radial gradient of metallicity (abundance of elements heavier than hydrogen and helium) in the Milky Way (*23*–*25*).

The age of classical Cepheids is correlated with their pulsation period, metallicity, and stellar rotation (*24*). Using the period distribution, we performed an age tomography of the Milky Way Cepheids (Fig. 3A). After applying the period-age relations for Cepheids (*24*) and including the metallicity gradient (*10*, *25*), we determined that the majority of Cepheids in our sample formed between 50 million and 250 million years (Ma) ago (Fig. 3B). The spatial distribution of ages shows that the closer to the Galactic Center, the younger the Cepheids we observe (Fig. 3, C to E). The age distribution of Cepheids does not directly reflect

[1]Astronomical Observatory, University of Warsaw, 00-478 Warsaw, Poland. [2]Department of Astronomy, Ohio State University, Columbus, OH 43210, USA. [3]Department of Physics, University of Warwick, Coventry CV4 7AL, UK.
*Corresponding author. Email: dszczyg@astrouw.edu.pl (D.M.S.); udalski@astrouw.edu.pl (A.U.)

that of all stars present in the disk. For example, the absence of short-period Cepheids in the inner disk does not necessarily mean that older (less massive) stars are absent in that region, as the higher metallicity there would not have produced Cepheids in the older population.

The spatial distribution of Cepheids shows several distinct features (Fig. 3A). Because these features are located mainly in the area monitored by OGLE, where the Cepheid detection efficiency is high (*3*), they are most likely real, rather than the result of an observational bias. The most prominent feature is formed by Cepheids within an age range of 90 to 140 Ma (Fig. 3D). Traces of this arc-shaped overdensity were previously associated with the Sagittarius-Carina spiral arm (*26–29*). An additional small overdensity in this age range is connected with the Perseus arm.

Figure 1B also shows additional overdensities of Cepheids. Figure 3, C and E, shows the distribution of our Cepheids in the age ranges of 20 to 90 Ma and 140 to 260 Ma, respectively. There are three overdensities in the youngest bin and two in the oldest one. The youngest overdensities roughly correspond to the inner Galaxy spiral arms (Norma-Cygnus, Scutum-Crux-Centaurus, and Sagittarius-Carina), whereas for the oldest ones, possible associations with the Perseus and Norma-Cygnus/Outer arms are much less evident. Cepheids within individual overdensities have similar ages, suggesting a common origin in past star formation episodes.

We performed a simple simulation in which we selected stars from three age bins. Median age values in these three groups were 64, 113, and 175 Ma. Then we searched for a star formation episode in one or more of the spiral arms, which, after a given time (after the Galaxy has rotated), would produce the currently observed distribution of Cepheids. The results of this simulation are presented in Fig. 4, where each row focuses on one of the age bins.

Figure 4, A, D, and G, shows the current observed distribution of Cepheids. Figure 4, B, E, and H, presents the positions of the spiral arms as they were 64 Ma, 113 Ma, and 175 Ma ago, respectively, following an assumed rotational period of the spiral pattern equal to 250 Ma (*29*). At those moments and locations, we injected star formation episodes. Figure 4, C, F, and I, shows how those star formation regions would look now (after 64, 113, and 175 Ma, respectively), taking into account the typical velocity of disk stars (*30*). We require a low-velocity dispersion of Cepheids during their birth (8 km/s) to match the coherent overdensities we observe.

Even with these simple assumptions, we find a good match between the observed and simulated distributions of Cepheids in the shape of the overdensities, as well as in their internal dispersion. Cepheids that were formed in a spiral arm do not currently follow the exact location of that arm; this can be explained by the difference in rotation velocity between the spiral density waves and the stars. This is the most pronounced in the case of the oldest group (Fig. 4, G to I), where the overdensities fall between the Perseus and Norma-Cygnus/Outer arms, in which they were most likely formed, and in the Sagittarius-Carina–Perseus arm gap.

We have produced a three-dimensional map of the Milky Way based on a large number of individual Cepheids with measured distances. This represents the young stellar population that extends to about 20 kpc, covering a large portion of our Galaxy, thus illustrating the extent and shape of the young stellar disk. Our work shows that a simple model can reproduce the current distribution of the young stellar disk of the Milky Way with narrow patches of stars of similar age.

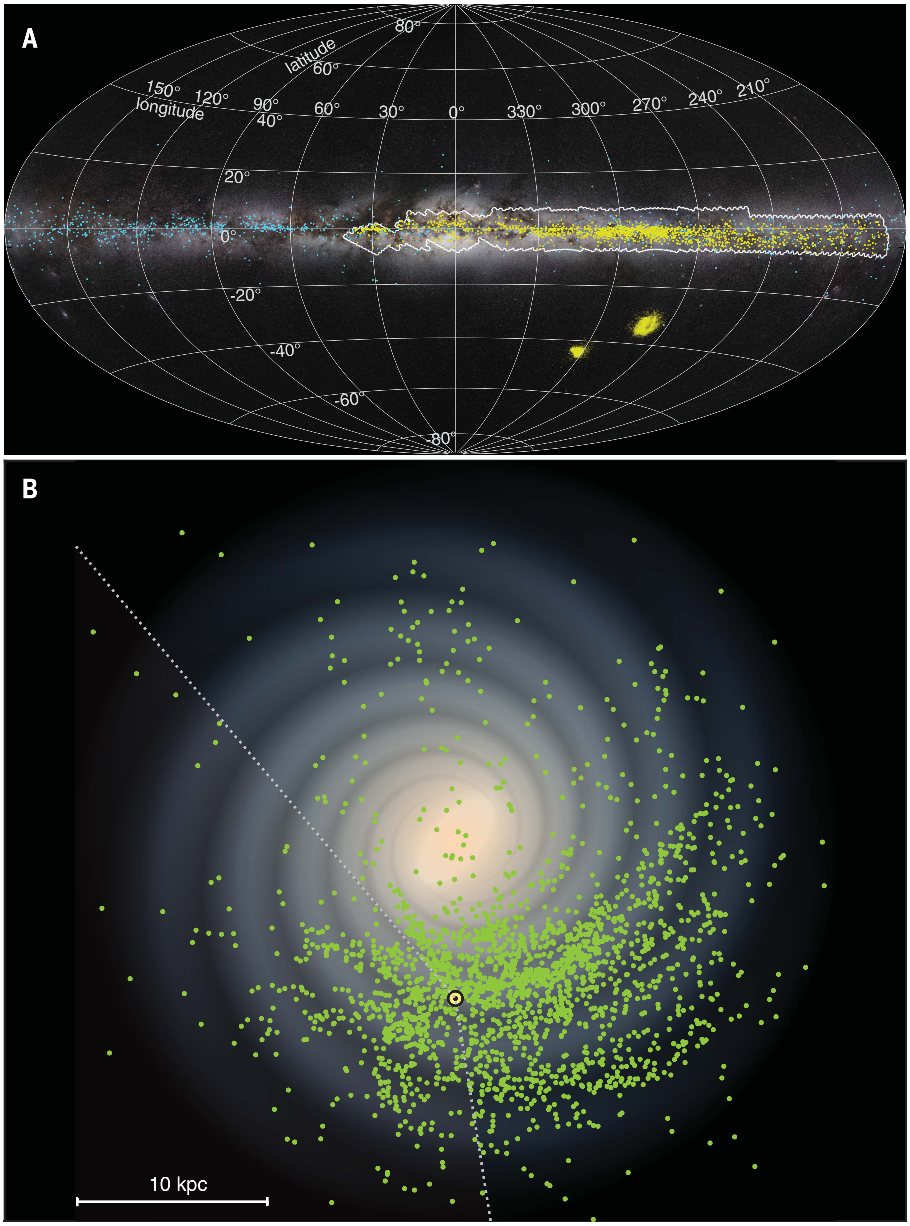


**Fig. 1. Distribution of galactic classical Cepheids.** (**A**) On-sky view of the Milky Way in galactic coordinates (*l*, *b*), with our sample of classical Cepheids in the Milky Way and in the Magellanic Clouds. Cepheids from the OGLE Collection of Variable Stars are shown with yellow dots, other sources with cyan dots (*10*). The white contour marks the OGLE survey area in the galactic plane (190° < *l* < 360°, 0° < *l* < 40°; −6° < *b* < +6°). The background image is a Milky Way panorama [by Serge Brunier; used with permission (ESO/S. Brunier)]. (**B**) Face-on view of our Galaxy with all 2431 Cepheids in our sample marked with green dots. The background image represents a four-arm spiral galaxy model consistent with neutral hydrogen measurements in our Galaxy [with the spiral structure modeled as logarithmic spirals (*29*)]. The Sun is marked with a yellow dot; the dashed lines show the angular extent of the OGLE fields (190° < *l* < 360°, 0° < *l* < 40°).

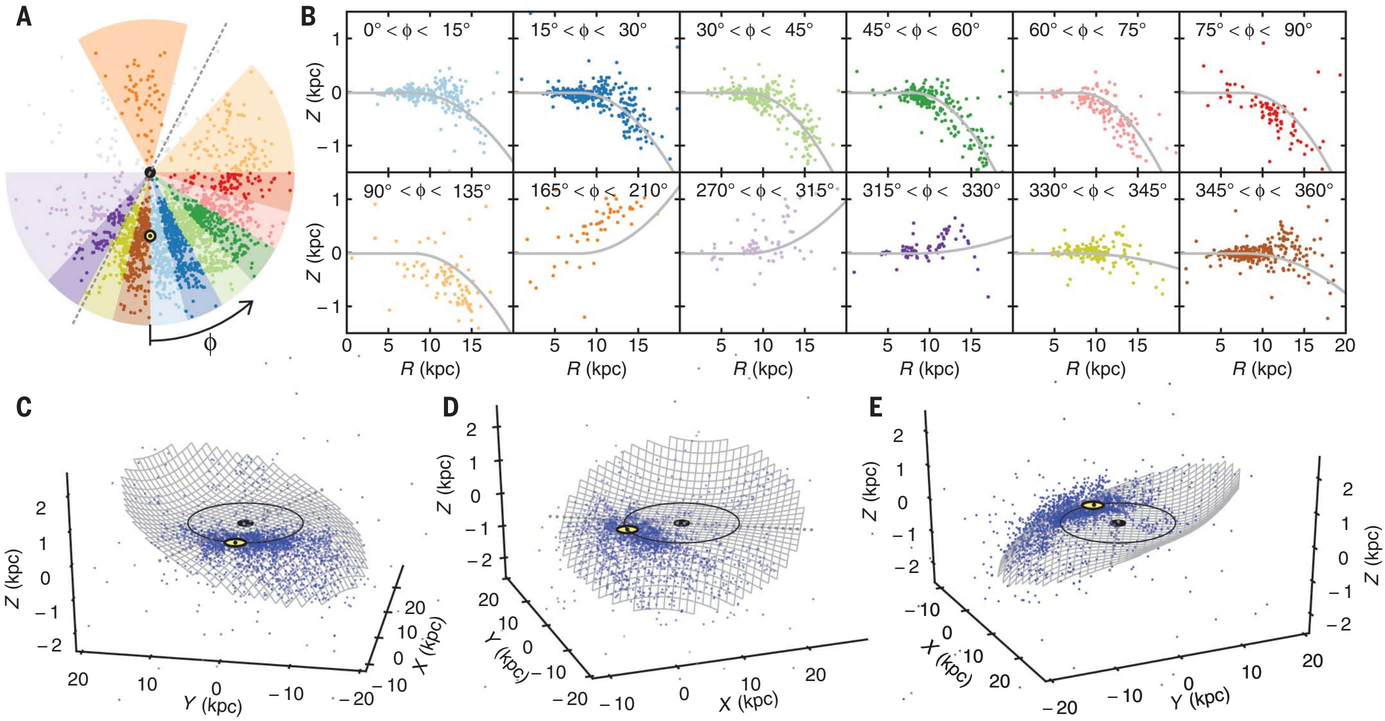


**Fig. 2. Warping of the Milky Way's disk.** (**A**) Top view of the galactic disk divided into 12 sectors in the galactocentric polar coordinate system. The azimuth ϕ = 0° is pointing to the Sun. The Sun is marked with a yellow dot, the Galactic Center with a black dot. Each sector is shown in a different color and is analyzed in (B). The dotted line on the disk separates parts of the Galaxy warped toward negative and positive *Z* (i.e., the line of nodes). (**B**) Distribution of Cepheids as a function of the galactocentric distance *R* versus distance from the galactic plane *Z* in each sector. The range of azimuth for each sector is labeled. Colors correspond to colors of the sectors in (A). Gray lines are positions of the model surface [(C) to (E)] within a given sector. (**C** to **E**) Model of the Milky Way warp from three viewing angles. Cepheids are marked with blue dots; the gray grid is a model surface fit to the Cepheid distribution (*10*). The Cartesian galactic coordinate system (*X*, *Y*, *Z*) is defined in (*10*). Vertical distances have been exaggerated by the choice of axes.

**Fig. 3. Ages of galactic classical Cepheids.** (**A**) Face-on view showing the Cepheid distribution in the Galaxy, with colors corresponding to Cepheid ages as indicated in (B). The Sun is marked with a yellow dot, the Galactic Center with a black dot. (**B**) Age histogram of galactic classical Cepheids in our sample. (**C** to **E**) Age tomography of the Milky Way Cepheids in three selected age bins, as indicated. Each age bin reveals Cepheid overdensities.

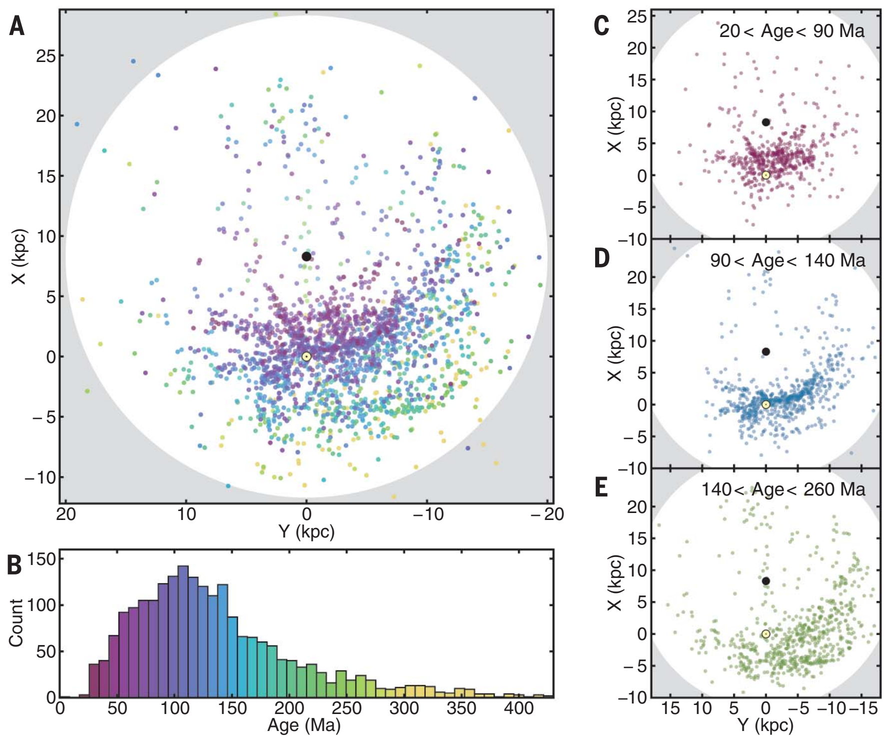

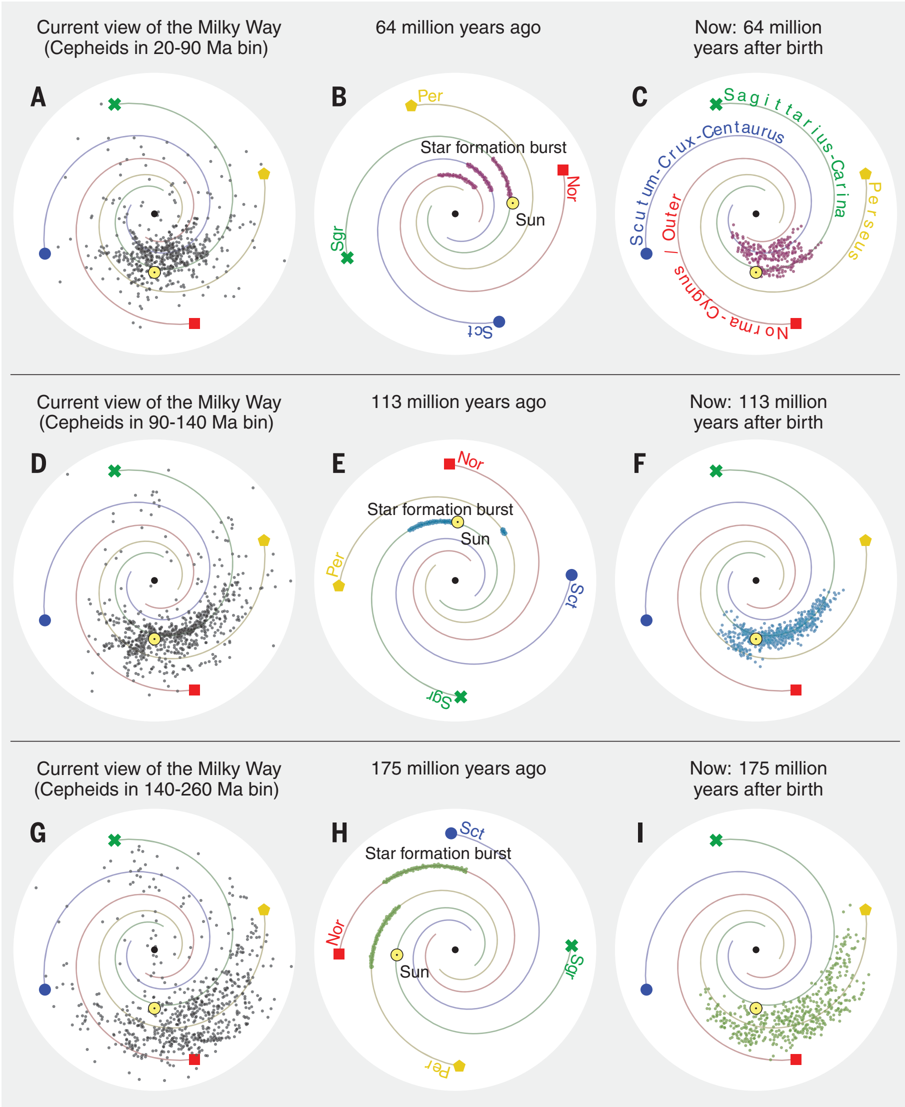


**Fig. 4. Possible origin of the Cepheid structures.** (**A**) Face-on view of our Galaxy, where Cepheids that belong to the age bin 20 to 90 Ma (median age 64 Ma) are shown with black dots. The Sun is marked with a yellow dot, the Galactic Center with a black dot. Locations of the spiral arms: yellow pentagon, Perseus arm; green cross, Sagittarius-Carina arm; blue dot, Scutum-Crux-Centaurus arm; red square, Norma-Cygnus/Outer arm. (**B**) Location of the Galaxy's spiral arms 64 Ma ago, with simulated star formation regions along the Norma-Cygnus/Outer, Scutum-Crux-Centaurus, and Sagittarius-Carina arms marked in violet. (**C**) Current location of stars from the simulated star formation region (violet). (**D** to **F**) Same as (A) to (C), but for the age bin 90 to 140 Ma with a median age of 113 Ma. (**G** to **I**) Same as (A) to (C), but for the age bin 140 to 260 Ma with a median age of 175 Ma.

## REFERENCES AND NOTES


1. H. S. Leavitt, E. C. Pickering, *Harvard College Observatory Circular 173* (1912).
2. A. Udalski, M. K. Szymański, G. Szymański, *Acta Astron.* **65**, 1–38 (2015).
3. A. Udalski *et al.*, *Acta Astron.* **68**, 315–339 (2018).
4. P. Pietrukowicz *et al.*, *Acta Astron.* **63**, 379–404 (2013).
5. N. N. Samus', E. V. Kazarovets, O. V. Durlevich, N. N. Kireeva, E. N. Pastukhova, *Astron. Rep.* **61**, 80–88 (2017).
6. G. Pojmański, *Acta Astron.* **52**, 397–427 (2002).
7. T. Jayasinghe *et al.*, *Mon. Not. R. Astron. Soc.* **477**, 3145–3163 (2018).
8. A. N. Heinze *et al.*, *Astron. J.* **156**, 241 (2018).
9. B. Holl *et al.*, *Astron. Astrophys.* **618**, A30 (2018).
10. See supplementary materials.
11. S. Wang, X. Chen, R. de Grijs, L. Deng, *Astrophys. J.* **852**, 78 (2018).
12. E. S. Levine, L. Blitz, C. Heiles, *Science* **312**, 1773–1777 (2006).
13. H. Nakanishi, Y. Sofue, *Publ. Astron. Soc. Jpn.* **55**, 191–202 (2003).
14. R. Drimmel, D. N. Spergel, *Astrophys. J.* **556**, 181–202 (2001).
15. M. López-Corredoira, A. Cabrera-Lavers, F. Garzón, P. L. Hammersley, *Astron. Astrophys.* **394**, 883–899 (2002).
16. Y. Momany *et al.*, *Astron. Astrophys.* **451**, 515–538 (2006).
17. C. Reylé, D. J. Marshall, A. C. Robin, M. Schultheis, *Astron. Astrophys.* **495**, 819–826 (2009).
18. E. B. Amôres, A. C. Robin, C. Reylé, *Astron. Astrophys.* **602**, A67 (2017).
19. D. J. Marshall, A. C. Robin, C. Reylé, M. Schultheis, S. Picaud, *Astron. Astrophys.* **453**, 635–651 (2006).
20. R. L. Smart, R. Drimmel, M. G. Lattanzi, J. J. Binney, *Nature* **392**, 471–473 (1998).
21. E. Poggio *et al.*, *Mon. Not. R. Astron. Soc.* **481**, L21–L25 (2018).
22. P. M. W. Kalberla, L. Dedes, J. Kerp, U. Haud, *Astron. Astrophys.* **469**, 511–527 (2007).
23. E. Antonello, D. Fugazza, L. Mantegazza, M. Stefanon, S. Covino, *Astron. Astrophys.* **386**, 860–864 (2002).
24. R. I. Anderson, H. Saio, S. Ekström, C. Georgy, G. Meynet, *Astron. Astrophys.* **591**, A8 (2016).
25. K. Genovali *et al.*, *Astron. Astrophys.* **566**, A37 (2014).
26. D. J. Majaess, D. G. Turner, D. J. Lane, *Mon. Not. R. Astron. Soc.* **398**, 263–270 (2009).
27. A. K. Dambis *et al.*, *Astron. Lett.* **41**, 489–500 (2015).
28. A. Sanna, M. J. Reid, T. M. Dame, K. M. Menten, A. Brunthaler, *Science* **358**, 227–230 (2017).
29. J. P. Vallée, *Astron. Rev.* **13**, 113–146 (2017).
30. P. Mróz *et al.*, *Astrophys. J.* **870**, L10 (2019).


## ACKNOWLEDGMENTS

We thank the reviewers for constructive comments that helped to improve the paper. This publication makes use of data products from the Wide-field Infrared Survey Explorer, which is a joint project of the University of California, Los Angeles, and the Jet Propulsion Laboratory/California Institute of Technology, funded by NASA. This work is based in part on observations made with the Spitzer Space Telescope, which is operated by the Jet Propulsion Laboratory, California Institute of Technology, under a contract with NASA. **Funding:** The OGLE project has received funding from the National Science Center (NCN), Poland, through grant MAESTRO 2014/14/A/ST9/00121 (A.U.). Also supported by NCN grant 2013/11/D/ST9/03445 (D.M.S.), NCN grant MAESTRO 2016/22/A/ST9/00009 (I.S.), and the Foundation for Polish Science–Program START (P.M.). **Author contributions:** D.M.S., J.S., and P.M. analyzed, modeled, and interpreted the galactic Cepheid data. A.U. initiated and supervised the project and prepared the sample of Cepheids. P.P. and I.S. made the final verification of the sample used in this analysis. M.K.S. provided positional data for Cepheid variables. D.M.S., J.S., P.M., and A.U. prepared the manuscript. All authors collected the OGLE photometric observations and reviewed, discussed, and commented on the results and on the manuscript. **Competing interests:** The authors have no competing interests. **Data and materials availability:** Data for our full Cepheid sample is available in table S1 and data S1. The OGLE Collection of Galactic Cepheids is available at the OGLE Archive: www.astrouw.edu.pl/ogle/ogle4/OCVS/. The Python code for the simulations shown in Fig. 4 is available at https://github.com/jskowron/galactic_cepheids.

## SUPPLEMENTARY MATERIALS

science.sciencemag.org/content/365/6452/478/suppl/DC1
Materials and Methods
Figs. S1 to S5
Tables S1 and S2
Data S1
References (*31*–*69*)

29 May 2018; accepted 5 July 2019
10.1126/science.aau3181

Science

# A three-dimensional map of the Milky Way using classical Cepheid variable stars

Dorota M. Skowron, Jan Skowron, Przemek Mróz, Andrzej Udalski, Pawel Pietrukowicz, Igor Soszynski, Michal K. Szymanski, Radoslaw Poleski, Szymon Kozlowski, Krzysztof Ulaczyk, Krzysztof Rybicki and Patryk Iwanek

*Science* **365** (6452), 478-482.
DOI: 10.1126/science.aau3181

**Cepheids help to map the Galaxy**

Cepheid variable stars pulsate, which allows their distances to be determined from the periodic variations in brightness. Skowron *et al.* constructed a catalog of thousands of Cepheids covering a large fraction of the Milky Way. They combined optical and infrared data to determine the stars' pulsation periods and mapped the distribution of Cepheids and the associated young stellar populations across the Galaxy. Their three-dimensional map demonstrates the warping of the Milky Way's disc. A simple model of star formation in the spiral arms reproduced the positions and ages of the Cepheid population.

*Science*, this issue p. 478